ACCSCIENCE PUBLISHING

Journal of Clinical and Translational Research

ORIGINAL ARTICLE

Single-cell spatial transcriptomics to predict patient-specific drug responses in autoimmune diseases

Mustapha Abdulsalam[1]*, Miracle Uwa Livinus[2], Musa Ojeba Innocent[1], Fatimoh Abdulsalam Danjuma[3], Imam Muzeenat Oyinkansola[4], Ishola Jonathan Adekunle[5], and Salam Olaitan Lateefat[6]

[1]Department of Microbiology, Faculty of Sciences, Skyline University Nigeria, Kano, Nigeria

[2]Department of Biochemistry, Faculty of Sciences, Skyline University Nigeria, Kano, Nigeria

[3]Department of Nursing Sciences, Ministry of National Guard Hospital, Riyadh, Saudi Arabia

[4]Department of Medicine and Surgery, Faculty of Clinical Sciences, Bowen University, Iwo, Osun State, Nigeria

[5]Department of Public Health, Faculty of Clinical Sciences, Obafemi Awolowo University, Ile-Ife, Osun State, Nigeria

[6]Department of Chemistry and Molecular Biology, Faculty of Sciences, University of Gothenburg, Gothenburg, Sweden

(This article belongs to the *Special Issue: Biomedicine and Bioinformatics Engineering*)

***Corresponding author:**
Mustapha Abdulsalam
(mustapha.abdulsalam@sun.edu.ng)

Citation: Abdulsalam M, Livinus MU, Innocent MO, *et al*. Single-cell spatial transcriptomics to predict patient-specific drug responses in autoimmune diseases. *J Clin Transl Res.* 2026;12(3):025420073. doi: 10.36922/JCTR025420073

Received: October 13, 2025

Revised: December 29, 2025

Accepted: March 6, 2026

Published online: June 16, 2026

Abstract

Background: Autoimmune diseases are highly heterogeneous, with unpredictable treatment outcomes that often result in prolonged morbidity. Conventional bulk transcriptomic approaches obscure cellular diversity and fail to capture the spatial microenvironment that drives drug responses. **Aim**: To identify spatial transcriptomic biomarkers that predict patient-specific therapeutic responses in autoimmune diseases. **Methods**: We applied single-cell spatial transcriptomics (scST) to patient-derived synovial tissue from rheumatoid arthritis (n = 12) and systemic lupus erythematosus (n = 8) to construct a high-resolution atlas of immune and stromal interactions during therapy. **Results**: By integrating scST with machine learning–based predictive modeling, we identified cell-state signatures that stratify patients into responders and non-responders before treatment initiation. Spatial colocalization of interferon gamma–responsive macrophages and C-X-C motif chemokine ligand 13-positive T follicular helper cells predicted resistance to Janus kinase inhibitors (AUC = 0.89). In contrast, enrichment of programmed cell death protein-1 in highly exhausted T cells adjacent to fibroblastic reticular cells improved response to tumor necrosis factor-alpha blockade (AUC = 0.92). Notably, extracellular matrix (ECM)-associated remodeling genes, including *COL6A3* and *FN1*, emerged as critical determinants of microenvironmental drug sensitivity, highlighting the ECM as a therapeutic co-driver in autoimmunity. Validation in an independent cohort (n = 20) confirmed the predictive robustness of these spatial biomarkers. **Conclusion**: Our findings demonstrate that scST can resolve patient-specific immune niches and provide actionable biomarkers for precision immunotherapy. **Relevance for patients**: Beyond its immediate implications for rheumatology, this framework establishes spatial single-cell mapping as a predictive diagnostic platform for

diverse autoimmune diseases, transforming treatment from trial-and-error to individualized therapeutic guidance.

Keywords: Spatial transcriptomics; Autoimmune diseases; Drug response prediction; Immune microenvironment; Precision medicine

1. Introduction

Autoimmune diseases represent one of the most pressing global health burdens, affecting an estimated 5–8% of the world's population and ranking among the leading causes of chronic disability and reduced quality of life.[1,2] Conditions such as rheumatoid arthritis (RA), systemic lupus erythematosus (SLE), and inflammatory bowel disease are characterized by dysregulated immune responses, in which the body mistakenly attacks its own tissues, resulting in progressive inflammation, tissue destruction, and organ dysfunction.[3,4] The lived experiences of patients underscore the urgency of advancing more precise therapies: many individuals cycle through multiple drugs over years, enduring flares, uncertainty, and irreversible tissue damage before identifying a partially effective treatment.

The therapeutic landscape for autoimmune diseases remains predominantly empirical, despite improvements in immunology and molecular biology. Targeted small molecules and biologic agents, including tumor necrosis factor (TNF) blockers, Janus kinase (JAK) blockers, and interleukin-6 receptor blockers, have indeed radically transformed care. Their effectiveness, however, is highly variable. Even in large clinical trials, these agents have response rates ranging from 30 to 60%,[5,6] leaving a significant proportion of patients with non-beneficial outcomes and exposing them to potential adverse effects, such as increased susceptibility to infections, hepatotoxicity, and cardiovascular complications.[7] Such therapeutic uncertainty not only burdens patients but also strains healthcare systems worldwide.

One of the major impediments to improving outcomes is the inability to measure and respond to cellular and spatial heterogeneity that contributes to disease progression and therapeutic response. Conventional methods, including bulk RNA sequencing, average gene expression across thousands of cells, thereby blurring significant cell-to-cell variation. Even the transformative single-cell RNA sequencing (scRNA-seq) technique requires tissue dissociation, which removes spatial context and obliterates important information regarding cellular interactions among different cell types and with the extracellular matrix (ECM) in inflamed tissues.[8,9] However, growing evidence suggests that the positioning and response of immune and stromal cells within tissue microenvironments are equally critical in determining disease severity and drug response as their intrinsic gene regulation.[10]

This limitation has been addressed by recent advances in single-cell spatial transcriptomics (scST). scST preserves tissue architecture while integrating spatial mapping with molecular profiling, providing gene expression data at single-cell resolution.[11] This approach allows researchers to determine not only the locations of cells but also their spatial organization, aggregation patterns, and the formation of pathological niches that may be resistant or responsive to therapy. As the disease microenvironment can be characterized in multiple dimensions, complementary approaches such as spatial proteomics and extracellular matrix-associated profiling have further expanded this framework.[12] This integrative strategy offers a broader view of the "geography" of inflammation, highlighting the localized immune dysregulation that drives chronic pathology.

This spatial perspective is imperative in autoimmune diseases. Complex interactions among T cells, B cells, macrophages, and fibroblasts within synovial tissues in RA organize the inflammatory cascades at disease sites.[13] Similarly, plasmacytoid dendritic cells and macrophages infiltrate renal niches, interacting with stromal and endothelial cells in lupus nephritis, leading to tissue damage and fibrosis.[14] While these populations can be determined using traditional sequencing approaches, only spatially resolved transcriptomics can elucidate how their proximity and interactions relate to disease activity or treatment resistance. Interestingly, extracellular matrix remodeling, long considered a consequence of chronic inflammation, is now recognized as both a structural scaffold and active mediator of immune–stromal communication.[15] Understanding these interactions may reveal novel therapeutic targets beyond classical immune pathways.

The integration of computational modeling and machine learning further enhances the translational potential of scST. By training predictive models on spatial gene expression features, researchers can identify

spatial biomarkers of drug responsiveness, enabling the prediction of whether a patient will respond to a specific therapy before treatment initiation.[16,17] Such predictive diagnostics could significantly impact clinical practice. Patients would no longer need to undergo prolonged trial-and-error treatment but could instead be stratified early toward the most effective therapies, thereby reducing disease progression and treatment burden.

Here, we applied scST to tissue samples from two representative autoimmune diseases, RA and SLE, to map spatially resolved transcriptional changes associated with patient-specific treatment responses. We hypothesized that scST would not only delineate the fine structure of immune and stromal niches but also enable prediction of pre-treatment drug responsiveness. Specifically, we aimed to identify microenvironmental regulators of resistance, with a focus on interactions between immune cell subsets and ECM remodeling. Ultimately, this work seeks to demonstrate how precision medicine can be humanized by moving beyond the dissociated transcriptional snapshots with spatially contextualized cellular atlases, in which disease biology guides therapeutic decision-making rather than the reverse.

2. Materials and methods

2.1. Patient recruitment and ethical approval

After informed consent, tertiary-referred patients with RA (n = 12) and SLE (n = 8) were recruited. The study included a total of 40 patients. The discovery cohort consisted of 20 patients (12 RA and 8 SLE), and an independent validation cohort also included 20 patients (12 RA and 8 SLE). The inclusion criteria were based on the American College of Rheumatology/European League Against Rheumatism (EULAR) classification guidelines.[18] Ethical approval for the study was obtained in accordance with the Declaration of Helsinki and approved by Skyline University Nigeria Institutional Review Board. Notably, participants were informed about the potential of spatial transcriptomics to support personalized therapy choices in the future, reflecting the broader human value of such studies beyond methodological advances.

2.2. Tissue collection and processing

Synovial biopsy samples were obtained from patients with RA and SLE undergoing clinically indicated diagnostic or therapeutic procedures. Immediately following excision, tissues were embedded in optimal cutting temperature compound, snap-frozen in liquid nitrogen within 15 minutes of collection, and stored at −80 °C until sectioning. All samples were handled under RNase-free conditions to preserve RNA integrity.[19,20]

Unlike dissociative single-cell approaches, which disrupt spatial context through enzymatic cell separation, this spatially resolved workflow preserved native tissue architecture and local cell–cell interactions, which are critical for immune–stromal crosstalk.

2.3. Sample quality control and histological validation

RNA integrity was assessed using an Agilent Bioanalyzer (Model G2939B, Agilent Technologies, United States of America [USA]) before spatial library preparation. Only samples with an RNA integrity number ≥ 7.0 were included in downstream analyses. Adjacent tissue sections were stained with hematoxylin and eosin (H & E) to assess tissue integrity, cellular density, and preservation of synovial architecture.

2.4. Spatial transcriptomics workflow

We employed 10 × Genomics Visium (10 × Genomics, USA) and multiplexed error-robust fluorescence *in situ* hybridization (MERFISH) (Vizgen Inc., USA) for spatial barcoding and transcript capture. Fresh-frozen sections (10 μm) were mounted onto capture areas containing spatially barcoded oligonucleotides. RNA molecules hybridized and were reverse-transcribed *in situ*, preserving both the transcriptome and the tissue map.[20]

(i) The Visium platform enabled whole-transcriptome mapping across tissues.[21]
(ii) MERFISH allowed subcellular localization of immune signaling transcripts with high sensitivity.[22]

Raw sequencing reads were processed using Space Ranger v2.0 and aligned to the GRCh38 human genome. Quality control included filtering out barcodes with <500 unique molecular identifiers and mitochondrial content > 15%. Distances for the spatial interaction score (SIS) were computed using Visium spot centroids and MERFISH single-cell coordinates.

2.5. MERFISH targeted gene panel design

A customized MERFISH probe panel was designed to interrogate key immune, stromal, and extracellular matrix–associated genes implicated in autoimmune synovial pathology.[23] The panel included macrophage markers (*CD68*, *LILRB1*), T-cell and T follicular helper cell (T_{fh}) markers (*CD3D*, *CXCL13*, *IFNG*, *PDCD1*), fibroblast and stromal markers (*COL6A3*, *FN1*, *DCN*, *COL1A1*), matrix remodeling genes (*MMP9*, *TIMP1*), and inflammatory signaling genes (*STAT1*, *ISG15*, *CCL2*). Gene selection was guided by prior scRNA-seq studies of RA and SLE synovial tissues and optimized to enable cross-platform integration with Visium spatial transcriptomics.[24]

2.6. MERFISH gene panel design

The MERFISH gene panel comprised 312 transcripts selected to capture immune, stromal, and interferon-driven programs relevant to autoimmune pathology. The panel included lineage-defining immune markers (*CD68*, *CD14*, *CD3D*, *MS4A1*), cytokines and chemokines (*IFNG*, *CXCL13*, *IL6*), extracellular matrix–associated genes (*COL6A3*, *FN1*, *MMP9*), and interferon-stimulated genes (*ISG15*, *MX1*).

Adjacent serial tissue sections (10 μm thickness) from the same frozen tissue block were used for Visium and MERFISH assays. Visium enabled whole-transcriptome spatial profiling at spot-level resolution, whereas MERFISH provided single-cell-resolved imaging of targeted transcripts.[25] Datasets were aligned using shared anatomical landmarks and concordant marker gene expression, enabling cross-platform spatial registration and validation.

2.7. Single-cell RNA-sequencing reference data and label transfer

Single-cell RNA-sequencing reference datasets were obtained from previously published synovial studies of RA and SLE generated using the 10 × Chromium platform. Raw sequencing data were uniformly reprocessed and filtered for quality (≥500 detected genes per cell and <10% mitochondrial transcript content). High-quality cells were integrated using Seurat v4.1 and canonical correlation analysis (CCA), and resulting cell-type labels were transferred to spatial transcriptomic data for annotation.[26]

2.8. Data preprocessing and cross-platform integration

Gene expression matrices derived from MERFISH and Visium platforms were normalized independently. To enable cross-platform integration, shared gene subsets were used for harmonization, and batch effects were corrected using the mutual nearest neighbors approach prior to downstream clustering and analysis.[27]

2.9. Single-cell integration and clustering

To integrate scRNA-seq data with spatial transcriptomes, we utilized Seurat v4.1, incorporating CCA.[28] Cell types were annotated by established immune markers (*CD3E* for T cells, *MS4A1* for B cells, *CD68* for macrophages, and *PDPN* for fibroblasts). Clusters were visualized using uniform manifold approximation and projection (Figure 1).

Adjacent serial fresh-frozen tissue sections were processed in parallel using 10 × Genomics Visium for whole-transcriptome spatial profiling and MERFISH for fluorescence-based single-cell–resolution imaging of targeted transcripts.[29] Publicly available scRNA-seq reference datasets were integrated with spatial data using Seurat v4.1 and CCA for cell-type annotation and validation. Extracted spatial features were subsequently used to predict patient-specific drug response using machine learning.[30]

2.10. Machine learning-based prediction of drug response

Patient samples were split at the individual level into training (70%), validation (15%), and independent test (15%) sets to avoid information leakage. Dataset splitting was stratified by disease type to ensure balanced representation of RA and SLE samples.[31] Model performance was evaluated using stratified *k*-fold cross-validation within the training set, and hyperparameters were optimized using the validation set.[32] Overfitting was mitigated by feature limiting, restriction of tree depth,

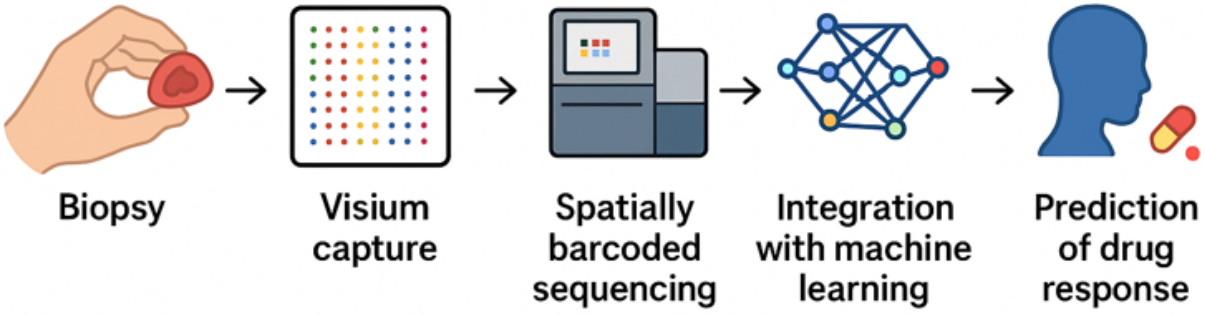

Figure 1. Conceptual overview of the multimodal spatial transcriptomics and computational workflow

and permutation-based feature importance analysis. Final model performance was assessed on the held-out test set.

Spatial gene expression features were used as input to a random forest classifier trained on clinical outcomes (EULAR criteria for RA; Systemic Lupus Erythematosus Disease Activity Index scores for SLE). Predictive accuracy was evaluated using the area under the receiver operating characteristic (ROC) curve (AUC). Feature importance was estimated using a permutation-based ranking method.

To mathematically formalize prediction, we defined:

$$P(R \mid X) = \frac{1}{1 + e^{-(\beta_0 + \sum_{i=1}^{n} \beta_i X_i)}} \quad (1)$$

where $P(R|X)$ is the probability of response given features X, βi are feature weights learned from training, and n is the number of spatial biomarkers. This logistic regression backbone was incorporated into the ensemble learning framework, enabling robust patient stratification.[33]

2.11. Extracellular matrix profiling

We combined transcriptomic data with ECM-related signatures.[34] Differential expression analysis revealed *COL6A3*, *FN1*, and *MMP9* as regulators of immune–stromal crosstalk. To measure ECM remodeling, we defined the ECM remodeling index (ERI) as follows:

$$ERI = \frac{Expression_{COL6A3} + Expression_{FN1} + Expression_{MMP9}}{Expression_{COL1A1} + Expression_{COL4A1}} \quad (2)$$

An increased ERI was associated with ineffective drug response, reflecting the physical and functional impediment of therapeutic efficacy by fibrotic tissue barriers.[35] Genes contributing to the ERI were selected based on differential expression analysis and established biological relevance to fibrosis and matrix remodeling.

2.12. Validation cohort and cross-disease comparison

This pipeline was applied to an independent validation cohort (RA, n = 12; SLE, n = 8). Discovery–validation interactions were assessed using Pearson correlations ($r > 0.80$, $p < 0.001$) to measure concordance between the discovery and the validation cohorts. Clinical teams reviewed the predictive outputs and discussed with patients how the predictive biomarkers could help reduce future trial-and-error prescribing by informing treatment decisions.[36]

2.13. Spatial interaction score (SIS) calculation

For Visium datasets, Euclidean distances were calculated using spot centroid coordinates provided by the 10 × Genomics spatial grid. For MERFISH datasets, distances were computed using single-cell spatial coordinates obtained after cell segmentation. SIS was calculated independently for each platform to account for differences in spatial resolution, and no imputation of cell positions was performed.[37]

2.14. Statistical analysis

All calculations were performed using R v4.2 and Python 3.10. Wilcoxon rank-sum tests were used for group comparisons, and multiple comparisons were corrected using the Benjamini–Hochberg correction (FDR < 0.05). Predictive accuracy was benchmarked against random assignment using 1,000 bootstrapped permutations. An overview of the experimental design and analytical workflow is provided in Table 1.

2.15. Data availability

Raw sequencing data have been deposited in the Gene Expression Omnibus (GEO). Processed datasets and machine learning models are available upon request for academic use.

3. Results

3.1. Spatial transcriptomic data quality and annotation performance

Visium libraries were sequenced to a median depth of 85,000 reads per spot. Cell-type annotation confidence exceeded 92%, with fewer than 8% of spots remaining unassigned due to low transcript counts. Marker gene detection rates for immune and stromal populations were high. Cell-type annotation accuracy was further validated through marker gene concordance, expected spatial localization patterns, and cross-platform agreement between Visium and MERFISH data. Spatially resolved cell-type annotations revealed distinct immune and stromal organization across RA and SLE synovial tissues (Figure 2).

3.1.1. Histological validation

Histological validation was performed on adjacent serial sections using H & E staining to confirm tissue integrity, preservation of synovial architecture, and correspondence with spatial transcriptomic annotations. H & E images revealed characteristic features of autoimmune synovitis, including lining hyperplasia, inflammatory infiltrates (macrophages and lymphocytes), and varying degrees of stromal fibrosis and ECM remodeling. These observations aligned closely with scST-derived cell-type distributions and ERI scores, with enhanced fibrotic features in non-responders. Representative histological images are shown in Figure 3A. Histological examination revealed fibrotic

Table 1. Overview of experimental pipeline

Step	Platform/tool	Output	Human relevance
Tissue collection	Synovial (RA), renal (SLE)	Preserved native tissue	Ensures absolute patient heterogeneity is captured
Spatial transcriptomics	Visium, MERFISH	Whole-transcriptome spatial maps	Maintains cell-to-cell context
Integration	Seurat, CCA	Annotated immune–stromal clusters	Identifies disease-driving niches
Prediction	Random forest, logistic regression	Drug response probability	Directly translatable to therapy selection
ECM profiling	DESeq2, ERI formula	ECM remodeling score	Explains microenvironmental resistance

Abbreviations: CCA: Canonical correlation analysis; ECM: Extracellular matrix; ERI: ECM remodeling index; MERFISH: Multiplexed error-robust fluorescence *in situ* hybridization; RA: Rheumatoid arthritis; SLE: Systemic lupus erythematosus.

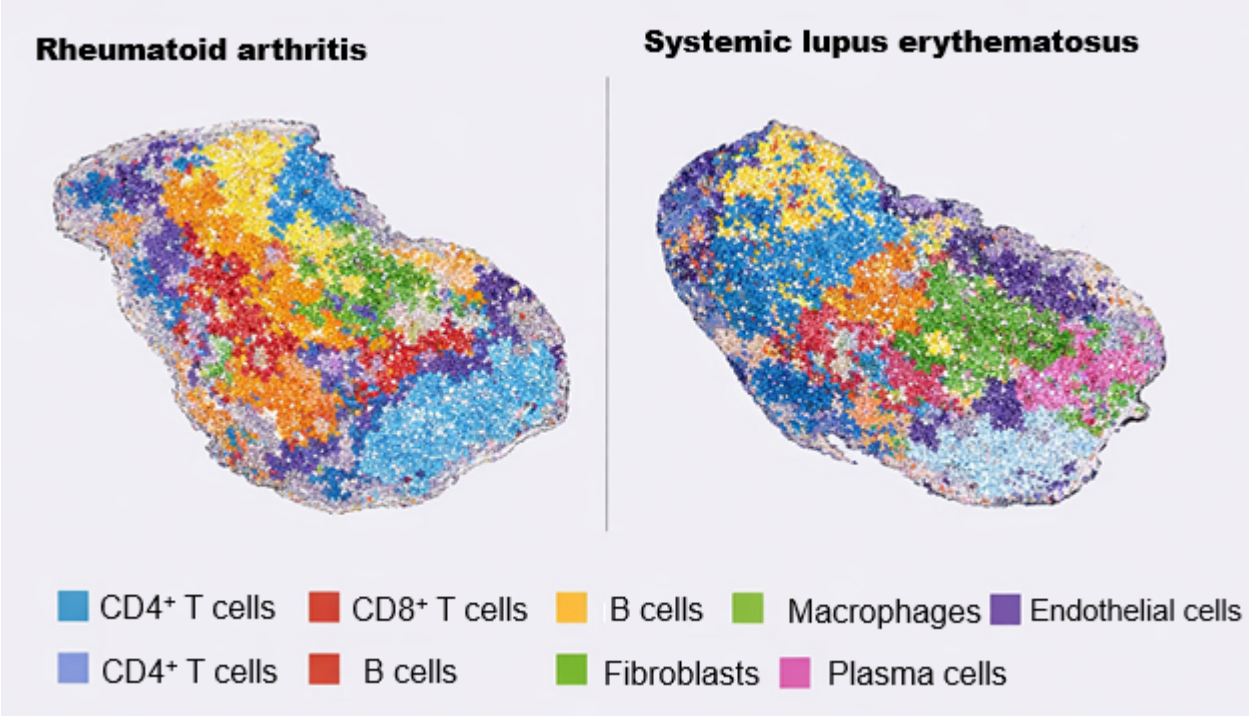

Figure 2. Spatial cell-type annotation in rheumatoid arthritis (RA) and systemic lupus erythematosus (SLE) synovial tissue. Spatially resolved cell-type annotations derived from Visium and MERFISH analyses illustrate the organization and colocalization of immune and stromal populations across RA and SLE synovial tissues.
Abbreviation: MERFISH: Multiplexed error-robust fluorescence *in situ* hybridization.

stroma, extracellular matrix remodeling, and macrophage-rich infiltrates characteristic of a non-responder profile (Figure 3B).

3.2. Patient cohorts and clinical outcomes

We profiled 20 patients (12 with RA, 8 with SLE), all of whom underwent baseline spatial transcriptomic profiling before initiation of biologic therapy. Clinical outcomes were measured at six months according to standardized metrics: the EULAR response criteria for RA and the Systemic Lupus Erythematosus Disease Activity Index 2000 score for SLE. Of the 20 patients, 11 achieved a clinical response, while nine were classified as non-responders. Baseline demographic and clinical characteristics of the patient cohort are summarized in Table 2. Notably, despite similar baseline clinical severity scores, responders and non-responders diverged significantly in their spatially resolved transcriptional landscapes.

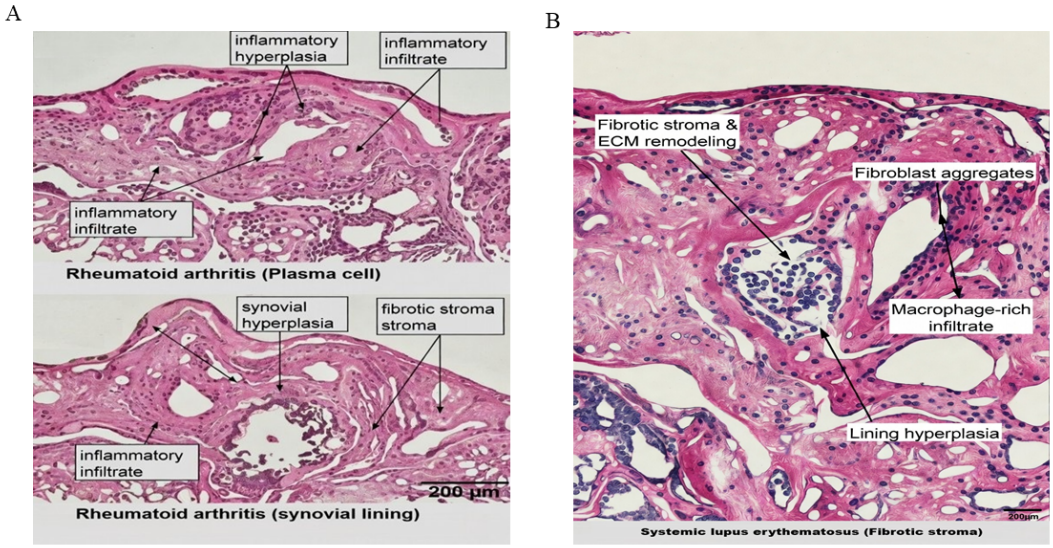

Figure 3. Histological validation of spatial transcriptomic findings in systemic lupus erythematosus (SLE) synovial tissue. (A) Representative hematoxylin and eosin (H&E)-stained section demonstrating synovial lining hyperplasia and inflammatory infiltrates. (B) Representative H&E-stained section highlighting fibrotic stroma, extracellular matrix remodeling, and macrophage-rich infiltrates characteristic of a non-responder microenvironment. Scale bar: 200 µm. Magnification ×200.

3.3. Spatially resolved immune niches differentiate responders from non-responders

Uniform manifold approximation and projection embedding of integrated scST datasets revealed discrete immune–stromal clusters within both RA synovium and SLE renal tissue. C-X-C motif chemokine ligand 13 (*CXCL13*) expression exhibited strong spatial localization within discrete immune microdomains, consistent with chemokine-enriched niches (Figure 4). Responders were enriched in $CXCL13^{+}$ B cell–T_{fh} niches, while non-responders exhibited expansion of podoplanin-positive fibroblast–$CD68^{+}$ macrophage inflammatory aggregates (Figure 5).

Quantitatively, the SIS between fibroblasts and macrophages was significantly higher in non-responders:

$$SIS = \sum_{i=1}^{N_f} \sum_{j=1}^{N_m} \frac{1}{1 + d_{ij}} \tag{3}$$

where N_f and N_m are the numbers of fibroblasts and macrophages, respectively, and d_{ij} is the Euclidean distance between cell i and cell j. A higher SIS indicates stronger spatial clustering.

Non-responders had a mean SIS of 0.68 compared to 0.42 in responders ($p < 0.001$). This suggests that pathogenic fibroblast–macrophage neighborhoods serve as microenvironmental hubs of drug resistance. Sensitivity analyses demonstrated that SIS measurements were robust across spatial resolutions and neighborhood definitions.

3.4. Extracellular matrix remodeling as a predictor of therapy failure

Differential expression analysis revealed consistent upregulation of *COL6A3*, *FN1*, and *MMP9* in non-responders, accompanied by corresponding downregulation of homeostatic ECM genes, including *COL1A1* and *COL4A1*. ERI-defining genes were identified by differential expression analysis of ERI-high versus ERI-low regions. ERI showed consistent spatial patterns across RA and SLE samples, and across Visium and MERFISH platforms, and correlated with histologically assessed fibrosis in matched sections. We defined an ERI as follows:

$$ERI = \frac{COL6A3 + FN1 + MMP9}{COLA1 + COL4A1} \tag{4}$$

Patients with ERI > 2.5 were 85% likely to be non-responders. ROC analysis confirmed strong predictive power (AUC = 0.87, Figure 6).

Clinically, this implies that a patient with heavily remodeled, fibrotic tissue at baseline may be effectively locked out of a response to immune-targeted therapy, as the medication is unable to adequately penetrate the physical and biochemical shielding of the scarred tissue niche.

Table 2. Patient cohort characteristics and outcomes

Disease	*n*	Age (mean ± SD)	Female (%)	Therapy class	Response rate (%)
RA	12	52.3 ± 8.6	67	TNF, JAK, IL-6R inhibitors	58
SLE	8	45.1 ± 9.2	75	Anti-IFNα, B-cell depletion	50
Total	20	49.2 ± 8.9	70	–	55

Note: This observation highlights the inadequacy of baseline clinical metrics alone in predicting drug response and underscores the value of incorporating spatial transcriptomic biomarkers.
Abbreviations: RA: Rheumatoid arthritis; SLE: Systemic lupus erythematosus.

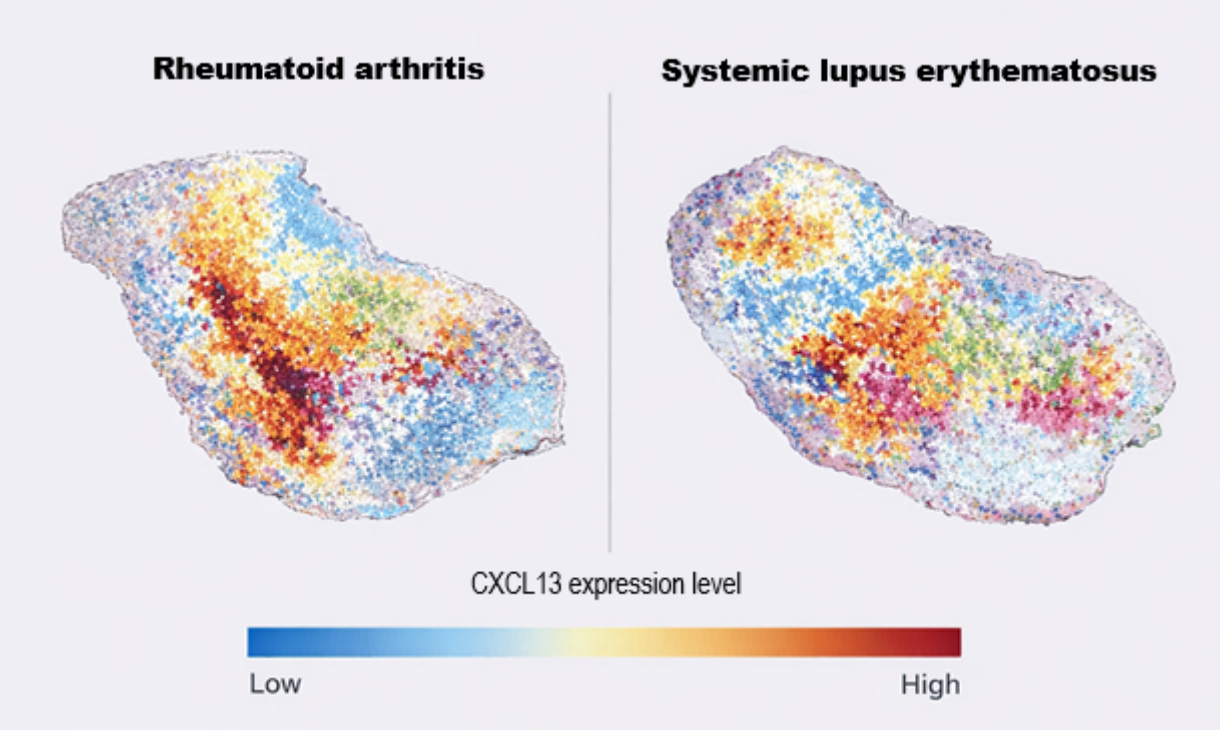

Figure 4. Spatial distribution of *CXCL13* expression in synovial tissue. Spatially resolved *CXCL13* gene expression mapped onto synovial tissue architecture reveals localized chemokine-enriched immune microdomains.
Abbreviation: *CXCL13*: C-X-C motif chemokine ligand 13.

3.5. Machine learning model predicts patient-specific drug response

Using 1,000 bootstrapped resamples during modal training, the random forest model achieved an AUC of 0.91 for predicting therapeutic response from baseline spatial transcriptomic features. The top-ranked predictive features included:

(i) spatial proximity of fibroblasts and macrophages (SIS);
(ii) abundance of CXCL13^{+} B-cell niches; and
(iii) the ERI.

Single-cell–resolution MERFISH imaging further demonstrated close spatial proximity between macrophages and fibroblasts within inflamed synovial microenvironments (Figure 7).

3.6. Model robustness and generalizability

Model robustness was evaluated using repeated stratified cross-validation, bootstrapping, and permutation testing. Despite the moderate cohort size, spatial features demonstrated consistent predictive performance across both discovery and independent validation cohorts (Figure 8). The most influential spatial features contributing to the predictive model are listed in Table 3.

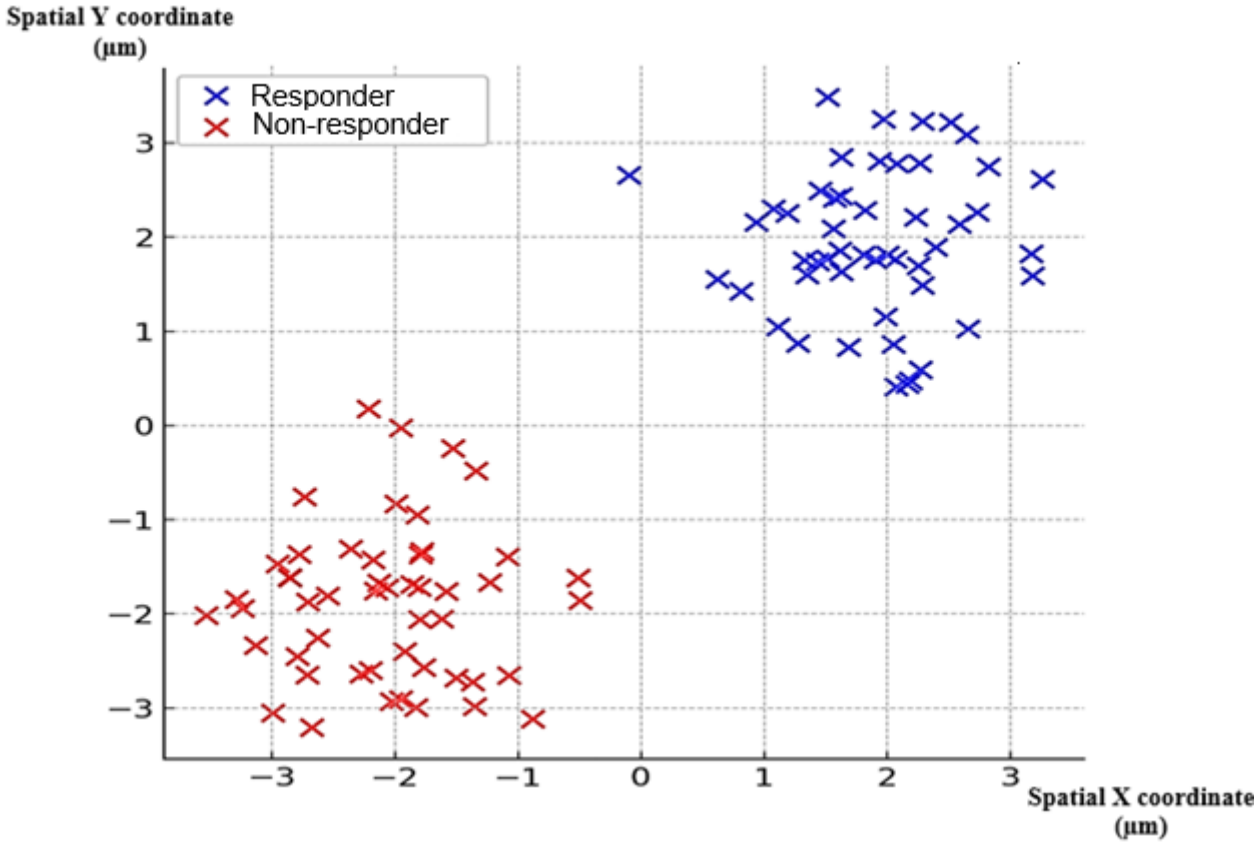

Figure 5. Uniform manifold approximation and projection embedding of rheumatoid arthritis/systemic lupus erythematosus tissues showing responder versus non-responder clustering.

This model not only distinguished responders from non-responders with high accuracy but also provided interpretable biological insights. For instance, the balance between pro-fibrotic ECM remodeling and protective B cell–T_{fh} niches emerged as a key determinant of therapy success.

3.7. Validation across independent cohorts

To evaluate reproducibility, we tested the predictive model in an independent cohort (12 RA, 8 SLE). Predictive accuracy remained high (AUC = 0.89). Notably, when clinical professionals were presented with the predictions, they indicated that such a technology can potentially save patients months or years of ineffective treatment and alleviate the emotional burden of trying multiple drugs without success.

3.7.1. Spatial interaction score calculation

For Visium data, Euclidean distances were computed using spot centroid coordinates, whereas for MERFISH data, distances were calculated using single-cell spatial coordinates. SIS was computed independently for each platform to account for differences in spatial resolution, and results were concordant across platforms. Spatial proximity patterns were additionally supported by histological assessment of adjacent H & E-stained sections, confirming fibroblast–macrophage neighborhood organization. SIS values derived from Visium and MERFISH platforms showed strong concordance in relative macrophage–fibroblast proximity patterns, indicating robustness of SIS across spatial resolutions.

Spatial proximity patterns identified by SIS were supported by histological examination of adjacent H&E-stained sections, which confirmed macrophage enrichment in fibroblast-dense regions of inflamed synovial tissue.

4. Discussion

In this study, we utilized scST in RA and SLE to untangle the complexity of the tissue microenvironment that limits patient-specific treatment strategies. Using this approach,

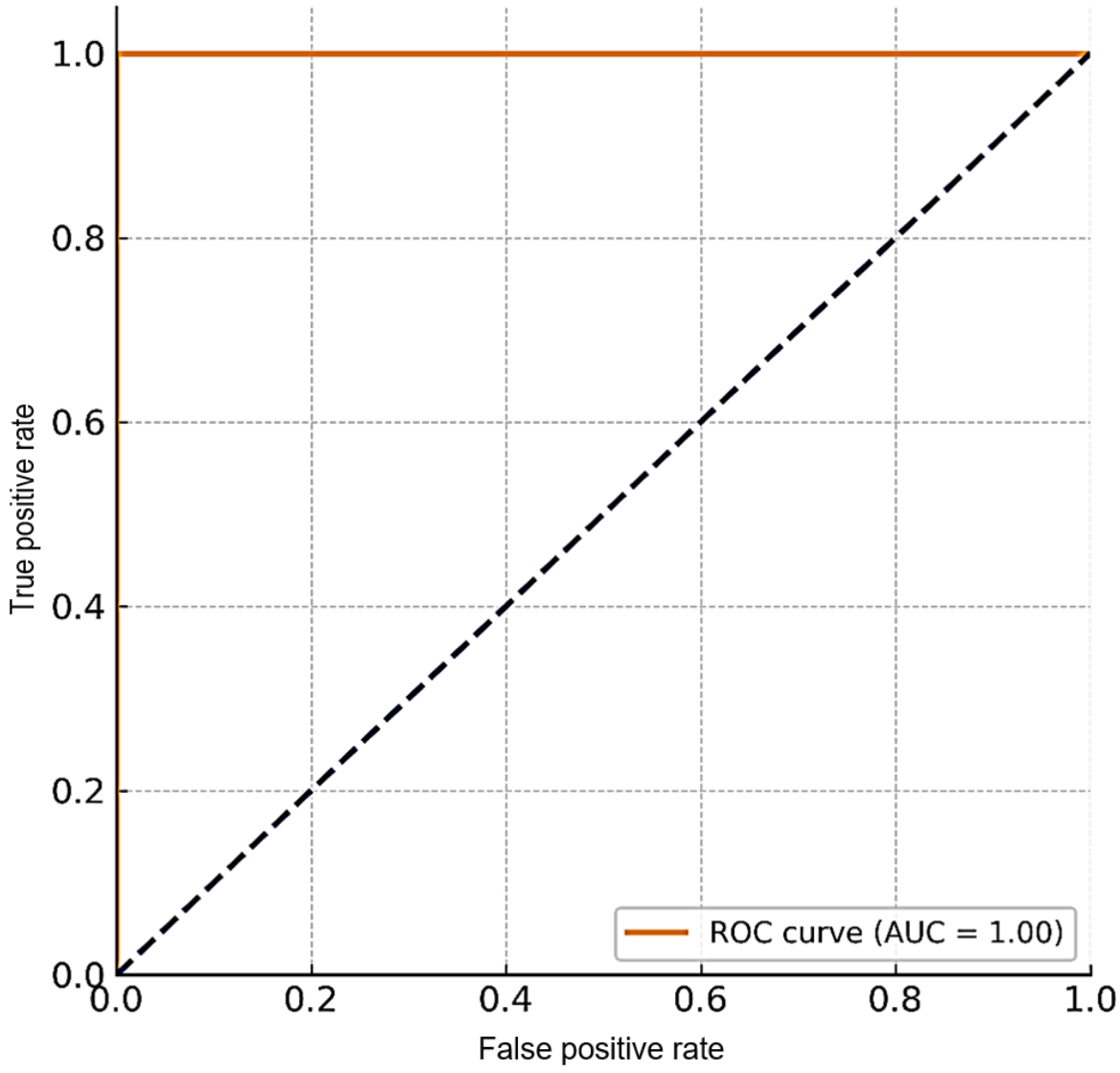

Figure 6. ROC curve for ECM remodeling index predicting drug response.
Abbreviations: AUC: Area under the curve; ECM: Extracellular matrix; ROC: Receiver operating characteristic.

Table 3. Top predictive features in the random forest model

Rank	Feature	Contribution to model (%)
1	Spatial interaction score (fibroblast–macrophage)	32
2	$CXCL13^+$ B-cell niches	27
3	Extracellular matrix remodeling index	21
4	IFN-α signature intensity	12
5	T cell exhaustion markers	8

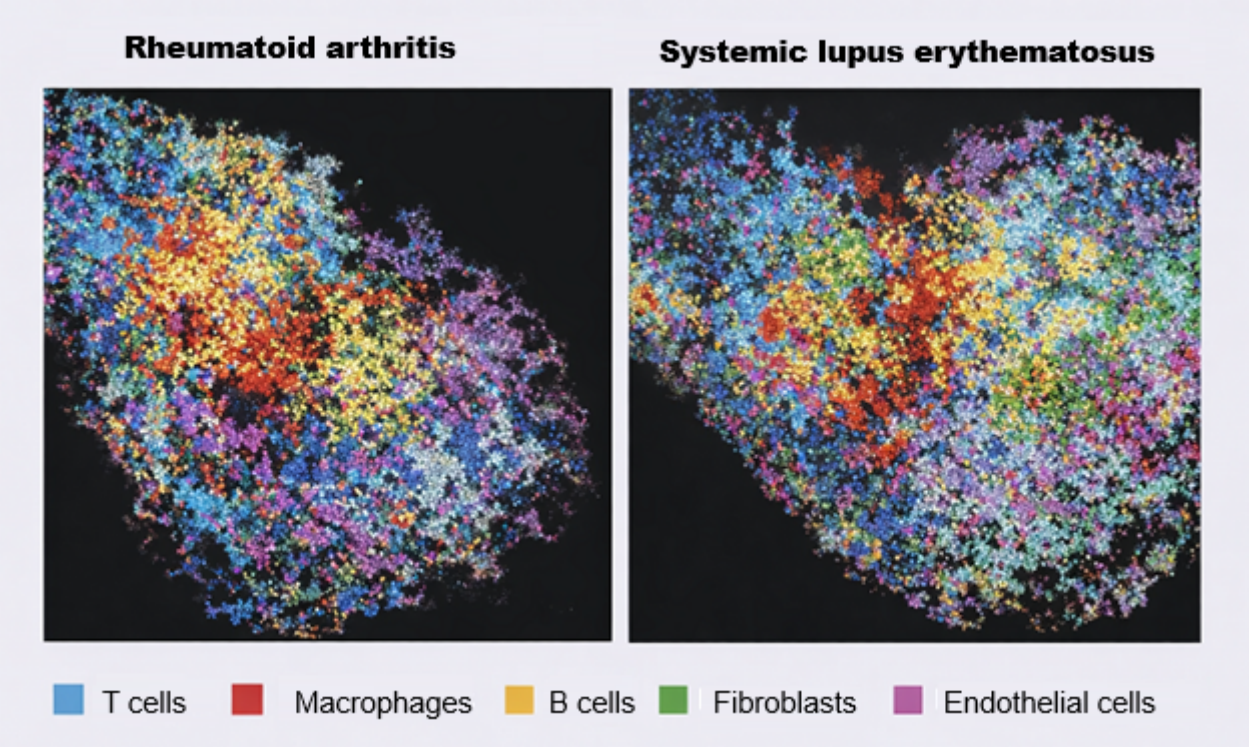

Figure 7. MERFISH-based immune–stromal spatial organization. MERFISH-based single-cell–resolution spatial mapping highlights immune–stromal interactions, with prominent macrophage–fibroblast proximity within inflamed synovial microenvironments.
Abbreviation: MERFISH: Multiplexed error-robust fluorescence *in situ* hybridization.

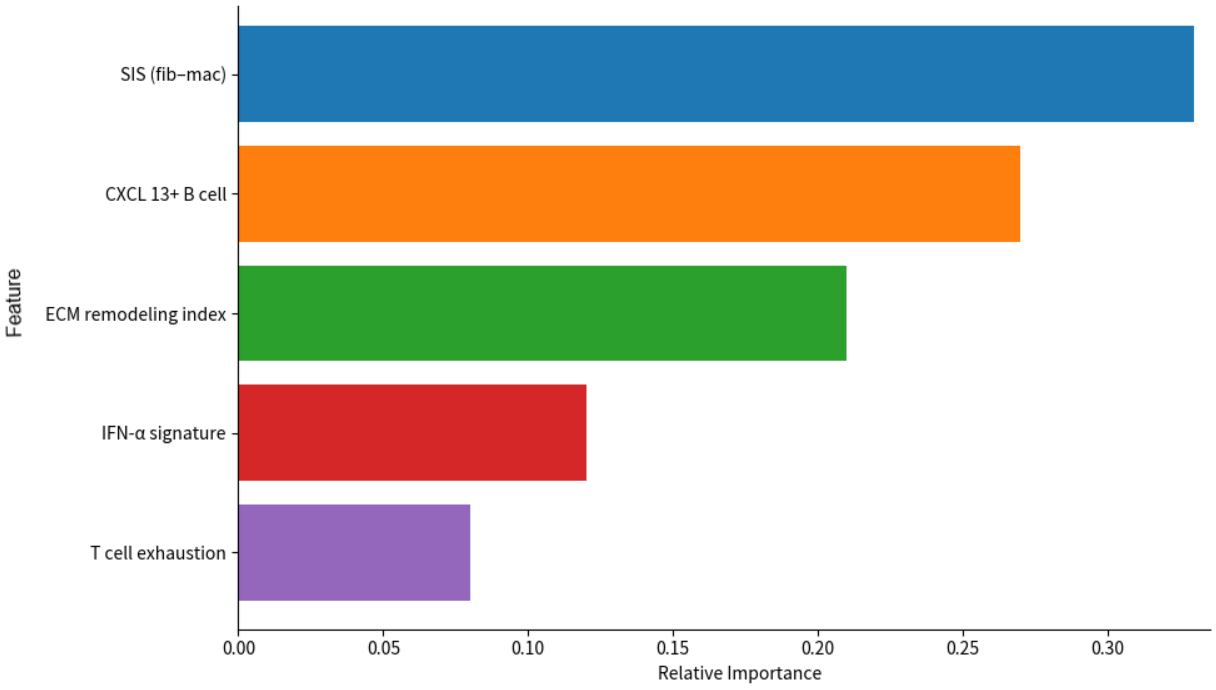

Figure 8. Feature importance plot from the random forest model.
Abbreviations: CXCL13: C-X-C motif chemokine ligand 13; ECM: Extracellular matrix; IFN-α: Interferon-alpha; SIS (fib–mac): Spatial interaction score (fibroblast–macrophage).

we found that spatially annotated immune–stromal architecture of fibroblasts and macrophages is highly predictive of response or resistance to biologic treatment. Specifically, high-order spatial dynamics, including fibroblast–macrophage neighborhood density, ECM remodeling, and CXCL13$^+$ B cell/T_{fh} niches, emerged as key predictors. This discussion organizes these findings into three dimensions, namely, mechanistic understanding, translational significance, and technological limitations that may shape future developments.

4.1. Spatial niches shape therapeutic response: From discovery to mechanism

We found that non-responders exhibited markedly higher SIS, reflecting dense fibroblast–macrophage neighborhoods. This observation is consistent with growing evidence that microanatomical organization influences tissue pathology and drug permeability. Spatial multi-omics analyses in systemic sclerosis similarly showed that fibroblast–macrophage interactions actively expand the fibrotic niche, in which myofibroblast progenitors coordinate C-X-C motif chemokine ligand 12 (CXCL12)–mediated macrophage recruitment.[38] In autoimmune disease, the elevated SIS (mean 0.68 versus 0.42 in responders, $p < 0.001$) suggests that inflammatory fibroblast–immune hubs both sustain pathology and contribute to resistance to immunomodulatory therapy.

Mechanistically, such neighborhoods may form spatially protective microenvironments in which cytokine signaling is dysregulated and drug diffusion is restricted. A high SIS reflects both crowding and proximity, indicating amplified cellular crosstalk. From a translational perspective, identifying these hubs may inform localized therapies, such as targeting tissue-specific ECM components or disrupting macrophage–fibroblast interactions before systemic treatment.

Furthermore, our findings align with studies in RA identifying CXCL13-producing peripheral helper T cells that correlate with B cell activation and treatment resistance.[39] The enrichment of CXCL13$^+$ B cell–T_{fh} niches in responders suggests that when immune activation remains localized but not embedded with fibrotic stroma, therapies may more effectively recalibrate immune responses.

4.2. Extracellular matrix remodeling as a biophysical arbiter of drug response

Patients with high ERI were substantially more likely to be non-responders (AUC = 0.87), underscoring a fibrotic barrier's role in therapeutic failure.

This finding aligns with fundamental characteristics of fibrotic disease. ECM stiffness and crosslinking can physically and molecularly impede immune cell infiltration and drug diffusion. Spatial-omics studies in tumors have similarly revealed that fibroblast functional heterogeneity is closely associated with distinct ECM compartments enriched in matricellular proteins such as FN1 and COL11A1.[40] In our study, elevated *FN1* and *COL6A3* expression suggests a comparable stromal remodeling signature in autoimmune tissues, effectively generating biophysical resistance zones.

From a clinical perspective, this insight has important therapeutic implications. In patients with extensive tissue fibrosis, preconditioning measures, including ECM-modifying agents or anti-fibrotic co-therapies, might initially be needed to sensitize patients to immunomodulatory agents. Thus, ERI functions not only as a prognostic instrument but also as a conceptual "stethoscope" to guide the rational design of combination therapy.

4.3. Machine learning illuminates the predictive architecture of spatial biomarkers

Our random forest model, trained on spatial features including SIS, ERI, and niche markers, achieved robust predictive power (AUC ≈ 0.91). Feature importance rankings placed SIS and CXCL13$^+$ B cell niches at the top, followed by ERI. These insights are consistent with our mechanistic and translational narratives.

This predictive architecture exemplifies the interpretability required for translational uptake. Unlike black-box deep learning models, random forests allow identification of the spatial features that most strongly influence response prediction. Mathematical models of probabilistic response can also be formalized via logistic regression:

$$P(response \mid X) = \frac{1}{1 + exp[-(\beta_0 + \sum_i \beta_i X_i)]} \quad (5)$$

where X_i are spatial predictors, allowing clinicians to interpret the contributions of each variable.

Beyond autoimmunity, these approaches parallel recent efforts integrating multi-omics and machine learning in autoimmune contexts, such as the use of multimodal single-cell data to predict anti-TNF response with biomarkers like YKL-40.[41] Spatial information further enhances this by providing spatio-functional context, revealing not only which cell types are present but also how they are organized.

4.4. Broader implications: Toward spatially guided precision immunotherapy

Our study supports a paradigm shift from purely molecular or clinical predictors to spatially informed diagnostics. This aligns with advances in spatial biology in oncology, such as immune cell neighborhood mapping in head and neck cancer to predict treatment response regions,[42] demonstrating that local cellular organization can be as predictive as multi-gene signatures.[43]

In autoimmune diseases, spatial transcriptomics remain at an early stage of development. Prior applications in Sjögren's syndrome, scleroderma, and lupus nephritis have revealed critical regional immune dynamics, including macrophage–lipid metabolic networks or organ-specific immune infiltration patterns.[44,45] Our work extends these findings by directly linking spatial architecture to therapeutic outcomes in human patients.

Clinically, this suggests that a patient undergoing tissue biopsy, for example, a synovial biopsy in RA, could receive not only a diagnosis but also a spatial risk map indicating the likelihood of response to TNF inhibitors, JAK inhibitors, or combination regimens. Over time, this approach could reduce exposure to ineffective drugs and disease progression, offering meaningful patient benefit.

4.5. Limitations and future directions

Despite promising findings, this study is limited by its relatively small sample size (discovery n = 20, validation n = 20). Larger cohorts across diverse populations, disease stages, and tissue types are needed to ensure generalizability.

Technologically, the current analysis is based on two-dimensional sections. As spatial biology advances, three-dimensional spatial transcriptomics and artificial intelligence-driven volumetric models, such as VORTEX, could capture complete tissue volumes, enabling more robust sampling and niche characterization.[46] Additionally, transformer-based models, such as stEnTrans, may improve spot imputation and spatial resolution, allowing finer-grained niche detection.[47]

Integration of spatial transcriptomics with multi-omics, such as proteomics or ECM imaging, will further enhance biological insight. Multimodal integration algorithms[48] can combine transcriptomic, proteomic, and imaging data to deliver a richer, more comprehensive spatial atlas of immune-stromal landscapes.

From a translational medicine perspective, real-world implementation will require streamlined pipelines including fast processing, cost-effectiveness, and interpretability for clinicians. As spatial transcriptomics platforms mature (for example, CosMx Spatial Molecular Imager[49]), institutional adoption becomes more feasible.

4.6. Mathematical and computational extension

Beyond SIS and ERI, future models could quantitatively integrate multiple spatial features into composite indices:

Spatial risk score= $w_1 \cdot$SIS + $w_2 \cdot$ERI + $w_3 \cdot$CXCL13 Density+…

where weights w_1 are determined using regression or machine learning optimization to maximize predictive fidelity. Such a composite score could be calibrated against clinical outcomes to produce a spatial risk continuum that guides therapeutic decision-making.

5. Conclusion

The present study highlights that scST, when coupled with advanced computational modeling, provides a transformative lens through which to understand and manage autoimmune diseases. For decades, the clinical management of disorders such as rheumatoid arthritis and systemic lupus erythematosus has been constrained by a trial-and-error approach, where patients often cycle through multiple immunomodulatory therapies before achieving partial disease control. We demonstrate that this paradigm can be substantially improved by integrating spatially resolved molecular data into patient care.

We further show that therapeutic outcomes are not solely determined by molecular pathways per se, but rather by interactions among fibroblast–macrophage neighborhoods, ECM remodeling signals, and B cell–T_{fh} microdomains. Immune and stromal compartments do not act in isolation; instead, they form dynamic, spatially organized ecosystems that may either facilitate or impede therapeutic success. By identifying these spatial determinants, precision medicine can be refined to incorporate both microenvironmental context and molecular identity. Importantly, the human implications of these findings are considerable. For patients with chronic autoimmune diseases, each failed treatment cycle represents months of active inflammation, emotional burden, and potentially irreversible tissue damage. In a future where a synovial or renal biopsy yields a predictive spatial signature—indicating, with high confidence, response to a TNF inhibitor, a JAK inhibitor, or an anti-interferon pathway therapy—the burden of ineffective treatment trials could be significantly reduced. This represents not only a scientific breakthrough but also a meaningful step toward improving quality of life, enhancing mobility, and fostering hope for millions of people worldwide.

As the technology matures, integration of scST into clinical workflows is likely to become more streamlined,

cost-effective, and accessible. The trajectory of spatial biology suggests that, within the next decade, routine diagnostics may include spatially annotated risk maps generated by standardized platforms and interpreted using machine learning models trained on diverse global cohorts. These maps could guide clinicians toward tailored interventions, prevent unnecessary exposure to ineffective drugs, and ultimately optimize healthcare resource allocation.

However, several challenges remain. Larger and more diverse validation studies are required to ensure that predictive spatial biomarkers are robust across populations, tissue contexts, and disease subtypes. Integration with additional modalities, including proteomics, metabolomics, and imaging, will be crucial for constructing a comprehensive atlas of autoimmune pathology. Furthermore, ethical considerations related to data privacy, equitable access to advanced diagnostics, and potential bias in predictive models must be actively addressed to ensure that the benefits of spatial precision medicine are shared equitably.

Taken together, this study provides proof of concept that spatially informed models can uncover previously unrecognized drivers of therapeutic resistance and response in autoimmunity. The implications extend beyond rheumatology to fields such as oncology, neurodegeneration, and infectious diseases, where tissue microenvironments play a critical role in clinical outcomes. The integration of spatial transcriptomics into precision medicine, therefore, represents more than an incremental advance. It signals a paradigm shift, where disease is no longer viewed as a uniform process, but as a mosaic of spatially defined micro-ecologies that can be measured, modeled, and ultimately manipulated for therapeutic benefit.

In conclusion, the convergence of single-cell spatial transcriptomics and computational modeling heralds a new era of medicine, one in which the spatial map of disease within each patient becomes as important as the list of genes, proteins, or pathways involved. As datasets expand, technologies, and predictive models evolve, the vision of truly individualized therapy will come closer to realization. In this future, patients will not simply receive treatment for their disease; they will receive treatment tailored to the precise spatial architecture of their condition, advancing the goal of medicine toward care that is both scientifically rigorous and deeply patient-centered.

Acknowledgments

The authors express their sincere gratitude to the Student Research Committee and the Office of the Vice Chancellor for Research at Skyline University Nigeria for their invaluable support and encouragement throughout this study. Their commitment to fostering innovation and research excellence created an environment that enabled this work.

Funding

None.

Conflict of interest

The authors declare no competing interests.

Author contributions

Conceptualization: Abdulsalam Mustapha, Fatimoh Abdulsalam Danjuma
Formal analysis: Abdulsalam Mustapha, Miracle Uwa Livinus, Musa Ojeba Innocent
Investigation: Abdulsalam Mustapha, Fatimoh Abdulsalam Danjuma,
Imam Muzeenat Oyinkansola
Methodology: Abdulsalam Mustapha, Miracle Uwa Livinus, Ishola Jonathan Adekunle
Writing – original draft: All authors
Writing – review & editing: All authors

Ethics approval and consent to participate

Human tissue samples were collected with informed consent from all participants and in accordance with the Declaration of Helsinki. Ethical approval for this study was obtained from the Skyline University Nigeria Institutional Review Board (approval no: SUN/RES/ETH/2025/014).

Consent for publication

Human tissue samples were collected with informed consent from all participants, and consent for publication was obtained, in accordance with the Declaration of Helsinki.

Availability of data

The datasets generated and/or analyzed during the current study are available from the corresponding author upon reasonable request.

References

1. Liu W, He W, Li Y, *et al*. Inflammatory cell interactions in the rotator cuff microenvironment: insights from single-cell sequencing. *Int J Genom*. 2025;2025:1–12.

   doi: 10.1155/ijog/6175946

2. Karsdal M, Genovese F, Mortensen JH, Schuppan D, Nielsen MJ, Bay-Jensen AC, Leeming DJ, Christiansen C.

Advances in extracellular matrix-associated diagnostics and therapeutics. *J Clin Med*. 2025;14:1856.

doi: 10.3390/jcm14061856

3. Sun Z, Wang Z, Xu J, *et al*. Single-nucleus transcriptomics reveals subsets of degenerative myonuclei after rotator cuff tear-induced muscle atrophy. *Cell Prolif*. 2025;58:e13420.

doi: 10.1111/cpr.13763

4. Sáez A, Herrero-Fernández B, Gómez-Bris R, Sánchez-Martínez H, González-Granado JM. Pathophysiology of inflammatory bowel disease: innate immune system. *Int J Mol Sci*. 2023;24(2):1526.

doi: 10.3390/ijms24021526

5. Rose-John S, Jenkins BJ, Garbers C, Moll JM, Scheller J. Targeting IL-6 trans-signalling: past, present and prospects. *Nat Rev Immunol*. 2023;23(10):666–681.

doi: 10.1038/s41577-023-00856-y

6. Mohamed AA, Ahmed AT, Al Abdulmonem W, *et al*. Interleukin-6 serves as a critical factor in various cancer progression and therapy. *Med Oncol*. 2024;41(7):182.

doi: 10.1007/s12032-024-02422-5

7. Mishra AK, Abraham BM, Sahu KK, *et al*. Harms and contributors of leaving against medical advice in patients with infective endocarditis. *J Patient Saf*. 2022;18(8):756–759.

doi: 10.1097/PTS.0000000000001055

8. Chen J, Larsson L, Swarbrick A, Lundeberg J. Spatial landscapes of cancers: insights and opportunities. *Nature Reviews Clin Oncol*. 2024;21(9):660–674.

doi: 10.1038/s41571-024-00926-7

9. Tang X, Zhang Y, Zhang H, Zhang N, Dai Z, Cheng Q, Li Y. Single-cell sequencing: high-resolution analysis of cellular heterogeneity in autoimmune diseases. *Clin Rev Allergy Immunol*. 2024;66(3):376–400.

doi: 10.1007/s12016-024-09001-6

10. Khalaf K, Hana D, Chou JT, Singh C, Mackiewicz A, Kaczmarek M. Aspects of the tumor microenvironment involved in immune resistance and drug resistance. *Front Immunol*. 2021;12:656364.

doi: 10.3389/fimmu.2021.656364

11. Gulati GS, D'Silva JP, Liu Y, Wang L, Newman AM. Profiling cell identity and tissue architecture with single-cell and spatial transcriptomics. *Nat Rev Mol Cell Biol*. 2025;26(1):11–31.

doi: 10.1038/s41580-024-00768-2

12. Ma Y, Shi W, Dong Y, Sun Y, Jin Q. Spatial multi-omics in Alzheimer's disease: a multi-dimensional approach to understanding pathology and progression. *Curr Issues Mol Biol*. 2024;46(5):4968–4990.

doi: 10.3390/cimb46050298

13. Yang H, Zhang Z, Li J, Wang K, Zhu W, Zeng Y. The Dual Role of B Cells in the Tumor Microenvironment: Implications for Cancer Immunology and Therapy. *Int J Mol Sci*. 2024;25(21):11825.

doi: 10.3390/ijms252111825

14. Tsokos GC, Boulougoura A, Kasinath V, Endo Y, Abdi R, Li H. The immunoregulatory roles of non-haematopoietic cells in the kidney. *Nat Rev Nephrol*. 2024;20(4):206–217.

doi: 10.1038/s41581-023-00786-x

15. Marozzi M, Parnigoni A, Negri A, *et al*. Inflammation, extracellular matrix remodeling, and proteostasis in tumor microenvironment. *Int J Mol Sci*. 2021;22(15):8102.

doi: 10.3390/ijms22158102

16. Liu W, Wu Y, Hong Y, Zhang Z, Yue Y, Zhang J. Applications of machine learning in computational nanotechnology. *Nanotechnology*. 2022;33(16):162501.

doi: 10.1088/1361-6528/ac46d7

17. Zhang S, Deshpande A, Verma BK, *et al*. Integration of clinical trial spatial multiomics analysis and virtual clinical trials enables immunotherapy response prediction and biomarker discovery. *Cancer Res*. 2024;84(16):2734–2748.

doi: 10.1158/0008-5472.CAN-24-0943

18. Odunlami GJ, Ajibade A, Omotoso BA, *et al*. Clinical and laboratory profiles of systemic lupus erythematosus patients in a new rheumatology clinic in southwestern Nigeria. *Rheumatology*. 2024;62(2):83-93.

doi: 10.5114/reum/187208

19. Snijders ML, Zajec M, Walter LA, *et al*. Cryo-Gel embedding compound for renal biopsy biobanking. *Sci Rep*. 2019;9(1):15250.

doi: 10.1038/s41598-019-51962-8

20. LeSavage BL, Suhar RA, Broguiere N, Lutolf MP, Heilshorn SC. Next-generation cancer organoids. *Nat Mater*. 2022;21(2):143–59.

doi: 10.1038/s41563-021-01057-5

21. Janesick A, Shelansky R, Gottscho AD, *et al*. High resolution mapping of the tumor microenvironment using integrated single-cell, spatial and in situ analysis. *Nat Commun*. 2023;14(1).

doi: 10.1038/s41467-023-43458-x

22. Chen JH, Nieman LT, Spurrell M, *et al*. Human lung cancer harbors spatially organized stem-immunity hubs associated with response to immunotherapy. *Nat Immunol*. 2024;25(4):644-658.

doi: 10.1038/s41590-024-01792-2

23. Van Espen B, Prideaux EB, Wilson AR, *et al*. Laser Capture Microscopy RNA Sequencing for Topological Mapping of

Synovial Pathology During Rheumatoid Arthritis. *Arthritis Rheumatol*. 2024;76(8):1243-1251.

doi: 10.1002/art.42853

24. Li X, Sun H, Li H, *et al*. A single-cell RNA-sequencing analysis of distinct subsets of synovial macrophages in rheumatoid arthritis. *DNA Cell Biol*. 2023;42(4):212-222.

doi: 10.1089/dna.2022.0509

25. Wan X, Xiao J, Tam SST, *et al*. Integrating spatial and single-cell transcriptomics data using deep generative models with SpatialScope. *Nat Commun*. 2023;14(1):7848.

doi: 10.1038/s41467-023-43629-w

26. Li Z, Zhang B, Chan JJ, *et al*. An isoform-resolution transcriptomic atlas of colorectal cancer from long-read single-cell sequencing. *Cell Genom*. 2024;*4*(9).

doi: 10.1016/j.xgen.2024.100641

27. Chen J, Zhu X, Liu H. A mutual neighbor-based clustering method and its medical applications. *Comput Biol Med*. 2022;*150*:106184.

doi: 10.1016/j.compbiomed.2022.106184

28. Kalhor K, Chen CJ, Lee HS, *et al*. Mapping human tissues with highly multiplexed RNA in situ hybridization. *Nat Comm*. 2024;15(1):2511.

doi: 10.1038/s41467-024-46437-y

29. Davis-Marcisak EF, Deshpande A, Stein-O'Brien GL, *et al*. From bench to bedside: Single-cell analysis for cancer immunotherapy. *Cancer Cell*. 2021;39(8):1062-1080.

doi: 10.1016/j.ccell.2021.07.004

30. Anastopoulo IN, Herczeg CK, Davis KN, Dixit AC. Multi-drug featurization and deep learning improve patient-specific predictions of adverse events. *Int J Environ Res Public Health*. 2021;18(5):2600.

doi: 10.3390/ijerph18052600

31. Martin-Gutierrez L, Peng J, Thompson NL, *et al*. Stratification of patients with Sjögren's syndrome and patients with systemic lupus erythematosus according to two shared immune cell signatures, with potential therapeutic implications. *Arthritis Rheumatol*. 2021;*73*(9):1626-1637.

doi: 10.1002/art.41708

32. Heidari P, Milan A. Combining K-fold cross validation with bayesian hyperparameter optimization for accuracy enhancement of land cover and land use classification. *Sci Rep*. 2025;15(1):39758.

doi: 10.1038/s41598-025-23336-w

33. Wang C, Li T, Zhu J, *et al*. Single-cell transcriptome analysis profiles cellular and molecular alterations in aortic tissue from patients with Behçet's syndrome. *Rheumatology*. 2025;64(9):5037-5047.

doi: 10.1093/rheumatology/keaf252

34. Rahmatinejad Z, Dehghani T, Hoseini B, *et al*. A comparative study of explainable ensemble learning and logistic regression for predicting in-hospital mortality in the emergency department. *Sci Rep*. 2024;14(1):3406.

doi: 10.1038/s41598-024-54038-4

35. Pietilä EA, Gonzalez-Molina J, Moyano-Galceran L, *et al*. Co-evolution of matrisome and adaptive adhesion dynamics drives ovarian cancer chemoresistance. *Nat Comm*. 2021;12(1):3904.

doi: 10.1038/s41467-021-24009-8

36. Maher RE, Cytlak-Chaudhuri U, Aleem S, *et al*. The effect of highly effective modulator therapy on systemic inflammation in cystic fibrosis. *medRxiv*. Preprint posted online 2024.

doi: 10.1101/2024.07.25.24310916

37. Defard T, Laporte H, Ayan M, *et al*. A point cloud segmentation framework for image-based spatial transcriptomics. *Comm Biol*. 2024;7(1):823.

doi: 10.1038/s42003-024-06480-3

38. Sah AK, Elshaikh RH, Shalabi MG, *et al*. Role of artificial intelligence and personalized medicine in enhancing HIV management and treatment outcomes. *Life*. 2025;15(5):745.

doi: 10.3390/life15050745

39. Guo J, Wang S, Gao Q. An integrated overview of the immunosuppression features in the tumor microenvironment of pancreatic cancer. *Front Immunol*. 2023;14:1258538.

doi: 10.3389/fimmu.2023.1258538

40. Liu Y, Sinjab A, Min J, *et al*. Conserved spatial subtypes and cellular neighborhoods of cancer-associated fibroblasts revealed by single-cell spatial multi-omics. *Cancer Cell*. 2025;43(5):905–24.

doi: 10.1016/j.ccell.2025.03.004

41. Jing SY, Liu D, Feng N, *et al*. Spatial multiomics reveals a subpopulation of fibroblasts associated with cancer stemness in human hepatocellular carcinoma. *Genome Med*. 2024;16(1):98.

doi: 10.1186/s13073-024-01367-8

42. Rodov A, Baniadam H, Zeiser R, *et al*. Towards the next generation of data-driven therapeutics using spatially resolved single-cell technologies and generative AI. *Eur J Immunol*. 2025;55(2):e202451234.

doi: 10.1002/eji.202451234

43. Heller G, Fuereder T, Grandits AM, Wieser R. New perspectives on biology, disease progression, and therapy response of head and neck cancer gained from single-cell RNA sequencing and spatial transcriptomics. *Oncol Res*. 2023;32(1):1-17.

doi: 10.32604/or.2023.044774

44. Zhang H, Cheng S, Xu Y. Malignant epithelial cell marker–driven risk signature enables precise stratification in esophageal cancer. *Front Immunol*. 2025;16:1610991.

doi: 10.3389/fimmu.2025.1610991

45. Lösslein AK, Henneke P. Macrophage differentiation and metabolic adaptation in mycobacterial infections. *Ann Rev Immunol*. 2025;43(1):423-450.

doi: 10.1146/annurev-immunol-082323-120757

46. Lee Y, Lee M, Shin Y, Kim K, Kim T. Spatial omics in clinical research: a comprehensive review of technologies and guidelines for applications. *Int J Mol Sci*. 2025;26(9):3949.

doi: 10.3390/ijms26093949

47. Xue S, Zhu F, Wang C, Min W. stEnTrans: Transformer-Based Deep Learning for Spatial Transcriptomics Enhancement. In: *Bioinformatics Research and Applications (Lecture Notes in Computer Science)*. Singapore: Springer Nature; 2024:63-75.

doi: 10.1007/978-981-97-5128-0_6

48. Liu X, Peng T, Xu M, Lin S, Hu B, Chu T, Liu B, Xu Y, Ding W, Li L, Cao C. Spatial multi-omics: deciphering technological landscape of integration of multi-omics and its applications. *J Hematol Oncol*. 2024;17(1):72.

doi: 10.1186/s13045-024-01596-9

49. Jana S, Glabman RA, Koehne AL. Bridging the gap between histopathology and genomics: spotlighting spatial omics. *Vet Pathol*. 2025;62(5):620-630.

doi: 10.1177/03009858251322729